C2 domain membrane penetration by group IVA cytosolic phospholipase A$_2$ induces membrane curvature changes[s]

Katherine E. Ward,* James P. Ropa,* Emmanuel Adu-Gyamfi,*,† and Robert V. Stahelin[1],*,†,§

Department of Chemistry and Biochemistry* and the Eck Institute for Global Health,† University of Notre Dame, South Bend, IN, 46556; and Department of Biochemistry and Molecular Biology,§ Indiana University School of Medicine-South Bend, South Bend, IN 46617

Abstract   Group IVA cytosolic phospholipase A$_2$ (cPLA$_2\alpha$) is an 85 kDa enzyme that regulates the release of arachidonic acid (AA) from the *sn*-2 position of membrane phospholipids. It is well established that cPLA$_2\alpha$ binds zwitterionic lipids such as phosphatidylcholine in a Ca^{2+}-dependent manner through its N-terminal C2 domain, which regulates its translocation to cellular membranes. In addition to its role in AA synthesis, it has been shown that cPLA$_2\alpha$ promotes tubulation and vesiculation of the Golgi and regulates trafficking of endosomes. Additionally, the isolated C2 domain of cPLA$_2\alpha$ is able to reconstitute Fc receptor-mediated phagocytosis, suggesting that C2 domain membrane binding is sufficient for phagosome formation. These reported activities of cPLA$_2\alpha$ and its C2 domain require changes in membrane structure, but the ability of the C2 domain to promote changes in membrane shape has not been reported. Here we demonstrate that the C2 domain of cPLA$_2\alpha$ is able to induce membrane curvature changes to lipid vesicles, giant unilamellar vesicles, and membrane sheets. Biophysical assays combined with mutagenesis of C2 domain residues involved in membrane penetration demonstrate that membrane insertion by the C2 domain is required for membrane deformation, suggesting that C2 domain-induced membrane structural changes may be an important step in signaling pathways mediated by cPLA$_2\alpha$.—Ward, K. E., J. P. Ropa, E. Adu-Gyamfi, and R. V. Stahelin. **C2 domain membrane penetration by group IVA cytosolic phospholipase A$_2$ induces membrane curvature changes.** *J. Lipid Res.* **2012.** 53: 2656–2666.

Supplementary key words   calcium • cytosolic phospholipase A$_2\alpha$ • lipid binding

Group IVA cytosolic phospholipase A$_2$ (cPLA$_2\alpha$) is an 85 kDa enzyme consisting of a N-terminal lipid-binding C2 domain (~120 residues) and a C-terminal catalytic or lipase domain (~600 residues) that is separated by a flexible linker (1, 2). cPLA$_2\alpha$ regulates arachidonic acid (AA) release from the *sn*-2 positions of membrane phospholipids; AA is used in the synthesis of leukotrienes and prostaglandins in response to inflammatory agonists (3). cPLA$_2\alpha$ has also been implicated in a number of pathological conditions, including asthma (4), cancers (5), arthritis (6), cerebral ischemia (7), and heart disease (8). The general principles governing cPLA$_2\alpha$ in vitro membrane binding (9, 10) and activation (11) as well as cellular translocation (12, 13) are well established, where the C2 domain binds with high affinity to zwitterionic membranes in a Ca^{2+}-dependent manner (9), whereas the catalytic domain binds to membranes independent of Ca^{2+} weakly (14). This functionality allows the C2 domain to act as a Ca^{2+} sensor in cells, which drives the cellular localization to the Golgi, ER, and nuclear membranes (2, 12, 13).

The C2 domain (~120 amino acids) contains three calcium-binding loops (CBLs), two of which (CBL1 and -3) harbor hydrophobic and aromatic amino acids (**Fig. 1**) that promote binding to zwitterionic membranes (9). Ca^{2+} binding induces a dramatic change in electrostatic potential, lowering the desolvation penalty associated with membrane insertion (15) and promoting the docking of the C2

Abbreviations: AA, arachidonic acid; ACCH, Amot coiled-coil homology domain; BAR, bin-amphiphysin-Rvs167; CBL, calcium binding loop; C1P, ceramide-1-phosphate; CD, circular dichroism; cPLA$_2\alpha$, group IVA cytosolic phospholipase A$_2$; EM, electron microscopy; ENTH, epsin N-terminal homology; FcR, Fc receptor; LUV, large unilamellar vesicle; PH, Pleckstrin homology; POPC, 1-palmitoyl-2-oleoyl-*sn*-glycero-3-phosphocholine; POPE, 1-palmitoyl-2-oleoyl-*sn*-glycero-3-phosphoethanolamine; POPS, 1-palmitoyl-2-oleoyl-*sn*-glycero-3-phosphatidylserine; SPR, surface plasmon resonance; TEM, transmission electron microscopy; WT, wild type.

[1] To whom correspondence should be addressed.
  e-mail: rstaheli@iupui.edu.
[s] The online version of this article (available at http://www.jlr.org) contains supplementary data in the form of one figure.
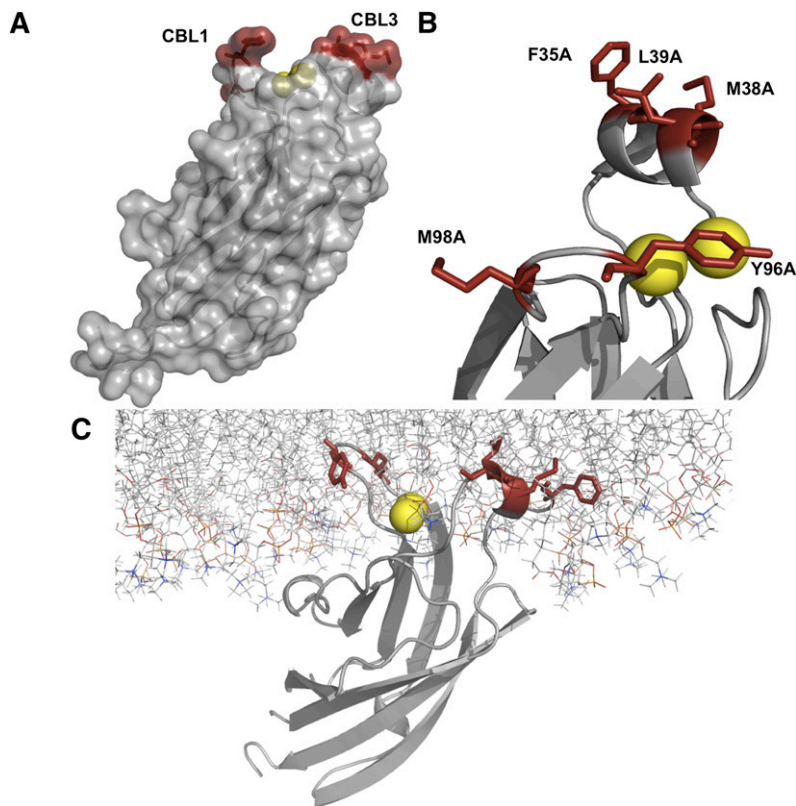
Fig. 1. Structural depiction of the C2 domain of cPLA$_2$α. A: The C2 domain (PDB ID 1CJY) is shown in gray in surface transparency mode to depict hydrophobic amino acids in calcium binding loops 1 and 3 (red). The two Ca^{2+} ions bound to the C2 domain are shown in yellow. B: A close-up view of the calcium-binding and membrane penetration regions of the C2 domain of cPLA$_2$α. Amino acids mutated in this study to assess membrane penetration and membrane curvature are shown in red (Phe^{35}, Met^{38}, and Leu^{39} in CBL1 and Tyr^{96} and Met^{98} in CBL3). Ca^{2+} ions crystalized with the protein are shown in yellow. C: The C2 domain has been shown to deeply penetrate zwitterionic membranes. Here the C2 domain is shown with the depth of penetration and orientation previously resolved by EPR (16) deeply penetrating hydrophobic and aromatic residues are shown in red (Phe^{35}, Met^{38}, and Leu^{39} in CBL1 and Tyr^{96} and Met^{98} in CBL3) and 2 Ca^{2+} ions in yellow. The domain was docked to the membrane according to previous biophysical studies, which provided molecular insight into the depth and orientation of the C2 domain binding to membranes (16). The protein shown is docked to a POPC membrane, which displays the importance of Phe^{35}, Met^{38}, and Leu^{39} in CBL1 and Tyr^{96} and Met^{98} in CBL3 in penetrating the lipid bilayer.

domain to the membrane bilayer. This penetration into the membrane has been shown to be significant, with a depth of ~15 Å (16), which extends extensively into the hydrocarbon region of the membrane. The significant membrane penetration of cPLA$_2$α is important for its membrane targeting to zwitterionic membranes and also to its ability to produce arachidonic acid. Recently, two anionic lipids—ceramide-1-phosphate (C1P) (17, 18) and PtdIns(4,5)P$_2$ (19, 20)—have been demonstrated to bind and activate cPLA$_2$α with emerging roles in the cellular translocation of the enzyme (21, 22).

Besides its role in eicosanoid biosynthesis, cPLA$_2$α is selectively activated upon Fc receptor (FcR)-mediated phagocytosis in macrophages, where it rapidly translocates to the nascent phagosome (23). Unexpectedly, however, it was shown that membrane binding by the isolated C2 domain of cPLA$_2$α was sufficient to induce phagosome formation (23), suggesting that the C2 domain alone has membrane binding activity that regulates phagocytosis. This was further verified with a mutation in the C2 domain, D43N, which abrogates Ca^{2+}-binding and could not rescue phagocytosis (23). cPLA$_2$α also plays a role in membrane curvature generation through regulation of aberrant Golgi vesiculation (24), Golgi tubulation (25), and vesiculation of cholesterol-rich, GPI-anchored, protein-containing endosomes (26). Although it is speculated the C2 domain may induce changes to membrane structure (23), direct evidence is lacking. These recent studies suggest that cPLA$_2$α and its C2 domain have membrane remodeling activity that is critical to biological signaling pathways.

Recently, a number of peripheral proteins, mainly attributed to their modular lipid binding domains, have been found to induce membrane curvature changes (27), including the epsin N-terminal homology (ENTH) (28), bin-amphiphysin-Rvs167 (BAR) (29), Pleckstrin homology (PH) (30), Amot coiled-coil homology domain (ACCH) (31), and C2 domains (32). Here, we investigate the ability of the isolated C2 domain of cPLA$_2$α to induce changes to lipid structure. A number of imaging assays are used, including electron microscopy (EM) of large unilamellar vesicles (LUVs), imaging of giant unilamellar vesicles (GUVs), and imaging of membrane sheets. In addition, biophysical assays, including monolayer penetration analysis and surface plasmon resonance (SPR), were used to correlate membrane penetration and affinity with membrane remodeling activity. Results provide evidence that Ca^{2+}-dependent membrane insertion of CBL1 and -3 of the C2 domain drive membrane curvature changes.

MATERIALS AND METHODS

Materials

1-palmitoyl-2-oleoyl-*sn*-glycero-3-phosphocholine (POPC), 1-palmitoyl-2-oleoyl-*sn*-glycero-3-phosphoethanolamine (POPE), and 1-palmitoyl-2-oleoyl-*sn*-glycero-3-phosphatidylserine (POPS) were purchased from Avanti Polar Lipids, Inc. (Alabaster, AL) and used without further purification. Octyl glucoside, (3-[3-cholamidopropyl) dimethylammonio]1-propane-sulfonate, Nunc Lab-Tek I Chambered Cover Glasses (8-well), and a bicinchoninic acid protein assay kit were from Thermo Fisher Scientific (Waltham, MA). L1 sensor chips were from GE Healthcare (Piscataway, NJ). *N*-(3-(triethylammoniumpropyl)-4-(4-(diethylamino)styryl)pyridinium dibromide (FM® 2-10) lipophilic dye was from Life Technologies (Grand Island, NY). Restriction endonucleases and enzymes for

molecular biology were obtained from New England Biolabs (Beverly, MA).

Cloning and protein expression

The QuikChange site-directed mutagenesis kit (Agilent Technologies, Santa Clara, CA) was used to introduce mutations into the pET28a vector with a His$_6$ tag engineered into the N-terminus of the cPLA$_2\alpha$ C2 domain gene (9). All mutated constructs were sequenced to ensure the presence of the desired mutation. The C2 domain and respective mutations were expressed and purified from *Escherichia coli* BL21(DE3) cells as previously described (9). Protein concentrations were determined by the bicinchoninic acid method, and all protein aliquots were stored in 20 mM HEPES (pH 7.4) containing 160 mM KCl.

Electron microscopy

Two hundred microliters of 1 mg/ml POPC LUVs were prepared as previously described (32). Briefly, the lipids were dried under nitrogen gas and resuspended in 20 mM HEPES (pH 7.4) containing 160 mM KCl and either 100 μM CaCl$_2$ or 100 μM EGTA. The vesicles were incubated at 37°C and extruded through an 800 nm filter (Avanti Polar Lipids, Alabaster, AL). The respective C2 domain and mutations were incubated at a concentration of 10 μM with the POPC vesicles for 30 min at 25°C. Samples were then applied to a carbon-formvar-coated copper grid and stained with 2% uranyl acetate. Liposome morphologies were then imaged at 80 kV on a FEI 80-300 D3203 electron microscope at 6,300× magnification.

Giant unilamellar vesicle assay

An aliquot of lipids containing POPC, POPE, and POPS suspended in chloroform were prepared in a 60:20:20 molar ratio. The suspension was dried under nitrogen gas and resuspended in chloroform to a final concentration of 0.4 mg/ml. The lipid suspension was dried onto an indium tin oxide-coated slide and dehydrated under a vacuum for 1 h. The GUV apparatus was assembled, and a 350 mM D-sucrose solution was placed into the reservoir containing the dried lipids. Another glass plate was placed on top to eliminate air from the system, and then a sin wave generator was applied at 3V and 20 Hz for 5 h at 25°C. The GUV solution was collected and stored at 25°C until use. The GUV solution was diluted 20-fold in 20 mM HEPES (pH 7.4) containing 160 mM KCl and 10 μM FM® 2-10 lipophilic dye. Samples were prepared with 100 μM EGTA, 10 μM CaCl$_2$, or 500 nM CaCl$_2$ as necessary for experimental conditions. GUV vesiculation was assessed after a 5 min incubation with 2 μM or 500 nM cPLA$_2\alpha$-C2, 500 nM full-length cPLA$_2\alpha$, or 2 μM of respective mutants and was imaged via confocal microscopy (Zeiss LSM 710) on Nunc Lab-Tek I Chambered Cover Glasses (8 well) using a 63× 1.4 NA oil objective. Three replicates for each control or sample were quantified by counting 60–100 GUVs per replicate. The number of vesiculated GUVs was determined separately and compared with the total number of GUVs in each replicate. The degree of vesiculation was then expressed as a percentage, compared with the control, and quantified using an unpaired Student *t*-test.

Membrane sheets

Two microliters of 10 mM POPC was prepared in chloroform, spotted onto Nunc Lab Tek I (8 well) Chambered Cover Glasses, and dried under a vacuum. The lipid was rehydrated with 20 mM HEPES (pH 7.4) containing 160 mM KCl and 20 μM FM® 2-10 and allowed to rehydrate for 15 min. Samples were prepared with 100 μM EGTA or 100 μM CaCl$_2$ as necessary for experimental conditions. The experiments contained 2 μM cPLA$_2\alpha$-C2 or respective mutants and were subsequently imaged after a 15 min incubation with a confocal microscope (Nikon A1R-MP with a 100× 1.4 NA oil objective).

Monolayer penetration

Surface pressure (π) of solution in a circular Teflon trough (2 ml) was measured using a wire probe connected to a Kibron MicroTrough X (Kibron, Inc., Helsinki, Finland) as previously described (33). Phospholipid solution (2–8 μl) in hexane/ethanol (9:1 v/v) was spread onto 2 ml of subphase to form a monolayer with a given initial surface pressure (π$_0$). The subphase was stirred continuously at 30 revolutions/min with a small magnetic stir bar. After stabilization of the surface pressure of the monolayer (∼5 min), the protein solution (typically 10 μl) was injected into the subphase, and the change in surface pressure (Δπ) was measured as a function of time. Generally, the Δπ value reached a maximum after 20 min. The maximal Δπ value depends upon the protein concentration and reached saturation at cPLA$_2\alpha$-C2 > 1 μg/ml, as previously reported (34). Protein concentrations in the subphase are maintained above such values to ensure that the Δπ represents a maximal value. The Δπ versus π$_0$ plots were constructed from these measurements to obtain the x-intercept or critical pressure (π$_c$) defined as the value to which the protein penetrates (35).

SPR assays

All SPR measurements were performed at 25°C. A detailed protocol for coating the L1 sensor chip has been described elsewhere (34). Briefly, after washing the sensor chip surface, 90 μl of POPC vesicles were injected at 5 μl/min to give a response of 6,500 resonance units. An uncoated flow channel was used as a control surface. Under our experimental conditions, no binding was detected to this control surface beyond the refractive index change for the C2 domain of cPLA$_2\alpha$ as previously reported (18, 34). Each lipid layer was stabilized by injecting 10 μl of 50 mM NaOH three times at 100 μl/min. SPR measurements were done at the flow rate of 5 μl/min. To give an association time to reach saturation of binding signal (R_{eq}), 50–90 μl of protein in 10 mM HEPES (pH 7.4) containing 160 mM KCl, and 50 μM Ca^{2+} was injected (see Fig. 5C). The saturation responses for wild type (WT) and mutations were normalized where maximum WT saturation response was set to 1 to compare the binding capacity of WT versus mutations. The lipid surface was regenerated using 10 μl of 50 mM NaOH. Each of the sensorgrams was corrected for refractive index change by subtracting the control surface response from the binding curve. A minimum of three data sets was collected for each protein at a minimum of five different concentrations for each protein within a 10-fold range of K_d. R_{eq} values were then plotted versus protein concentration and the K_d value was determined by a nonlinear least-squares analysis of the binding isotherm using the equation $R_{eq} = R_{max}/(1 + K_d/C)$ (36). Each data set was repeated three times to calculate a standard deviation.

Circular dichroism spectroscopy

To ensure the WT and mutant proteins retained a stable structure, circular dichroism (CD) was used to assess the secondary structure of each recombinant protein used in the study. The spectra were taken on a JASCO 815 CD spectrometer scanned from 195 to 250 nm in a 1 mm quartz spectrophotometer cell (Starna Cells Inc., Atascadero, CA) at 20°C in 10 mM Hepes and 80 mM KCl (pH 7.4). Each measurement was performed in triplicate and averaged to yield the representative scans shown in supplementary Fig. IA. Molar ellipticity was defined according to the JASCO software and was subtracted from a control buffer

scan. WT and mutations displayed overlapping spectra consistent with β-sheet structure.

Calcium binding assay

To measure the calcium-binding capacity of WT cPLA$_2$α-C2 and the point mutants, the calcium detector Bis-Fura-2 (Life Technologies, Carlsbad, CA) was used according to the manufacture's protocol. Briefly, 2 μM protein was incubated for 30 min with control or 10 μM Ca^{2+} standard in a black fluorescent plate with a clear bottom (Costar Life Science, Tewksbury, MA). The difference in the unknown Ca^{2+} concentration was determined in relation to a standard curve by measuring the ratio of the emission at 510 nm at excitation wavelengths of 350 nm and 380 nm, respectively. Percent binding was normalized to the average WT binding capacity. Measurements were performed in triplicate for WT and mutations to determine the standard deviation (supplementary Fig. IB).

RESULTS

Electron microscopy of liposome morphology changes induced by the C2 domain

EM has been used to effectively characterize changes in liposome morphologies induced by the ENTH (28), BAR (29), ACCH (31), and C2 domains (32). To assess the ability of the C2 domain of cPLA$_2$α to induce changes to liposome morphologies, we used transmission EM (TEM) with negative staining to visualize liposomes before and after incubation with the C2 domain. The C2 domain induced dramatic changes in POPC liposome structures as long tubules were extensively visualized through the grids (**Fig. 2**). Moreover, the tubulation of liposomes induced by the C2 domain was Ca^{2+} dependent; experiments performed in the presence of 100 μM EGTA in place of CaCl$_2$ did not display detectable changes in liposome morphology (Fig. 2). The ENTH, BAR, and ACCH domains insert into the hydrocarbon region of the membrane bilayer, which is a prerequisite for their ability to induce membrane curvature changes (31, 37–39). To test if hydrophobic and aromatic residues, which typically insert into membranes, were required for liposome morphology changes, we prepared mutations of hydrophobic and aromatic residues in calcium binding loops 1 and 3 of the C2 domain (Fig. 1). Earlier studies have demonstrated the ability of these calcium-binding loops to penetrate deeply into membranes and monolayers where hydrophobic and aromatic residues in these loops protrude into the hydrocarbon region of the membrane (9, 16). Indeed, F35A/L39A and Y96A displayed a drastic reduction in liposome morphology changes and displayed a lack of long, thin tubules emanating from liposomes as seen for the WT C2 domain. M38A and M98A, which have been shown to have a lesser effect than F35A, L39A, or Y96A on cPLA$_2$ membrane binding (9), induced changes in liposome structure, albeit to a lesser extent than WT.

Quantification of membrane curvature changes using GUVs

GUVs have served as an effective platform for monitoring changes to membrane structure because they can be fluorescently labeled and imaged with confocal microscopy and are more easily quantified than EM experiments. GUVs have been effective in monitoring membrane curvature changes for the ENTH domain (37) and viral matrix proteins (40). In addition, they are relatively flat (mean diameter, ∼30 μM) in comparison to LUVs (mean diameter, ∼400 nm), so they can be used to assess if proteins induce membrane curvature changes on different membrane surfaces. GUVs composed of POPC:POPE:POPS (60:20:20) were prepared and used to quantify membrane curvature changes for WT C2 domain and respective mutations. All experiments were performed in triplicate, and at least 60 GUVs were counted in each experiment and assessed for membrane curvature changes in response to C2 domain binding. WT C2 domain induced vesiculation of GUVs in the presence of Ca^{2+}, which was not observed in the presence of 100 μM EGTA (**Fig. 3A**). The hydrophobic and aromatic mutations F35A/L39A and Y96A, which greatly reduced alterations to liposome morphology in the EM assays, significantly reduced GUV vesiculation for which their quantitative value was similar to that of the control. M38A and M98A displayed a statistically significant reduction in GUV vesiculation, in line with the EM assays, which detected appreciable changes to liposome structure, albeit to a lesser extent than WT. To assess the ability of the C2 domain to induce membrane curvature changes, we assessed the ability of the C2 domain to induce vesiculation in GUVs with 200 nM WT C2 domain
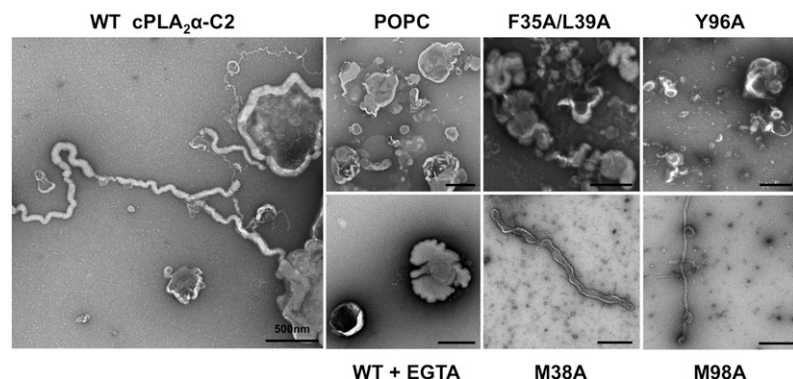

Fig. 2. The C2 domain induces membrane tubulation of POPC LUVs. Transmission electron microscopy was used to assess the ability of the C2 domain and mutants to induce changes to liposome morphology. All measurements were done with 10 μM protein in 20 mM HEPES (pH 7.4) containing 160 mM KCl and either 100 μM CaCl$_2$ or 100 μM EGTA. WT C2 induced extensive tubulation of POPC liposomes in a Ca^{2+}-dependent manner. However, mutations F35A/L39A and Y96A greatly reduced changes in liposome morphology, whereas M38A and M98A induced formation of tubules from liposomes but to a lesser extent than WT. Incubation of the C2 domain in 100 μM EGTA in place of CaCl$_2$ with POPC liposomes did not induce appreciable changes in liposome morphology. Scale bars = 500 nm.
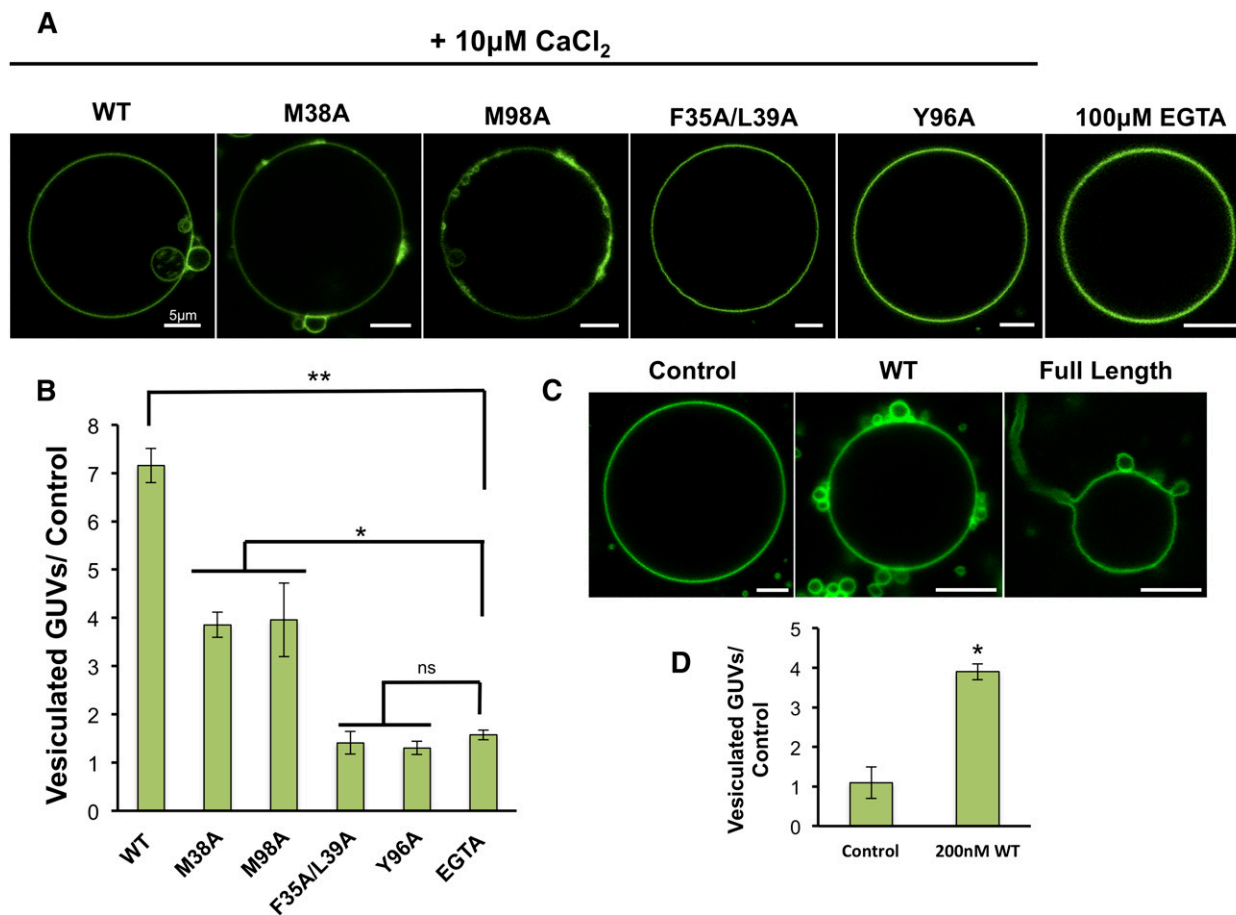
Fig. 3. The GUV assay demonstrates the C2 domain's ability to induce membrane budding. A: Experiments with POPC:POPE:POPS (60:20:20) GUVs were performed in triplicate with a minimum of 60 GUVs assessed per measurement to provide a quantitative representation of membrane curvature changes shown in B. B: Quantitative representation of GUV vesiculation induced by C2 domain and respective mutants. WT induced significant vesiculation of GUVs in the presence of 10 μM CaCl$_2$ compared with control experiments performed in 100 μM EGTA. M38A and M98A displayed some induction of GUV vesiculation and membrane reorganization but to a significantly lesser extent than WT. F35A/L39A and Y96A did not appreciably induce GUV vesiculation when compared with the control. C: The WT C2 domain and full-length cPLA$_2\alpha$ were assessed at 200 nM protein concentration for their ability to induce membrane curvature changes in the presence of 500 nM CaCl$_2$ to GUVs containing POPC:POPE:POPS (60:20:20). The WT C2 domain induced substantial vesiculation, whereas full-length cPLA$_2\alpha$ induced vesiculation and long tubule formation from GUVs. D: Quantification of vesiculation in control versus WT C2 experiments shown in C. The *P* value for each protein was determined in comparison to the control in C and D (ns, not significant; *P < 0.001; **P < 0.0001) using an unpaired Student *t*-test. Scale bars = 5 μm.

in the presence of 500 nM CaCl$_2$. Indeed, under these conditions, which are closer to physiological concentrations of cytoplasmic Ca^{2+}, the C2 domain induced substantial GUV vesiculation (Fig. 3C, D). We also assessed the ability of full-length cPLA$_2\alpha$ to induce membrane curvature changes to GUVs at 200 nM protein in the presence of 500 nM CaCl$_2$. The full-length enzyme not only induced GUV vesiculation but also prompted extensive tubulation emanating from the GUVs.

The C2 domain induces fragmentation of membrane sheets

Membrane sheets labeled with fluorescent dye, which represent a relatively flat membrane surface, have been used to image membrane curvature changes for the PH domain of FAPP1 and -2 (30). Here we used POPC membrane sheets labeled with FM® 2-10 dye to assess the ability of the C2 domain to induce changes to membrane sheet structure. Membrane sheets were imaged before

and after introduction of C2 domain and mutants to observe changes in real time (**Fig. 4A**). In the presence of Ca^{2+}, the C2 domain induced rapid fragmentation of POPC membrane sheets (Fig. 4A). The specific nature of this finding was confirmed by adding the same volume of protein storage buffer to ensure that changes in volume did not induce membrane swelling or membrane fragmentation. Additionally, mutations that greatly reduced membrane structural changes in the EM or GUV assays (F35A/L39A and Y96A) also abolished membrane fragmentation of POPC sheets (Fig. 4B). M98A displayed similar membrane fragmentation as WT C2, but M38A did not induce detectable changes in membrane sheet structure up to 25 min after the addition of protein. Taken together, these data indicate that the C2 domain is able to induce changes to membrane structure for small, highly curved membranes (LUVs) as well as less curved and relatively flat membranes (GUVs and membrane sheets).
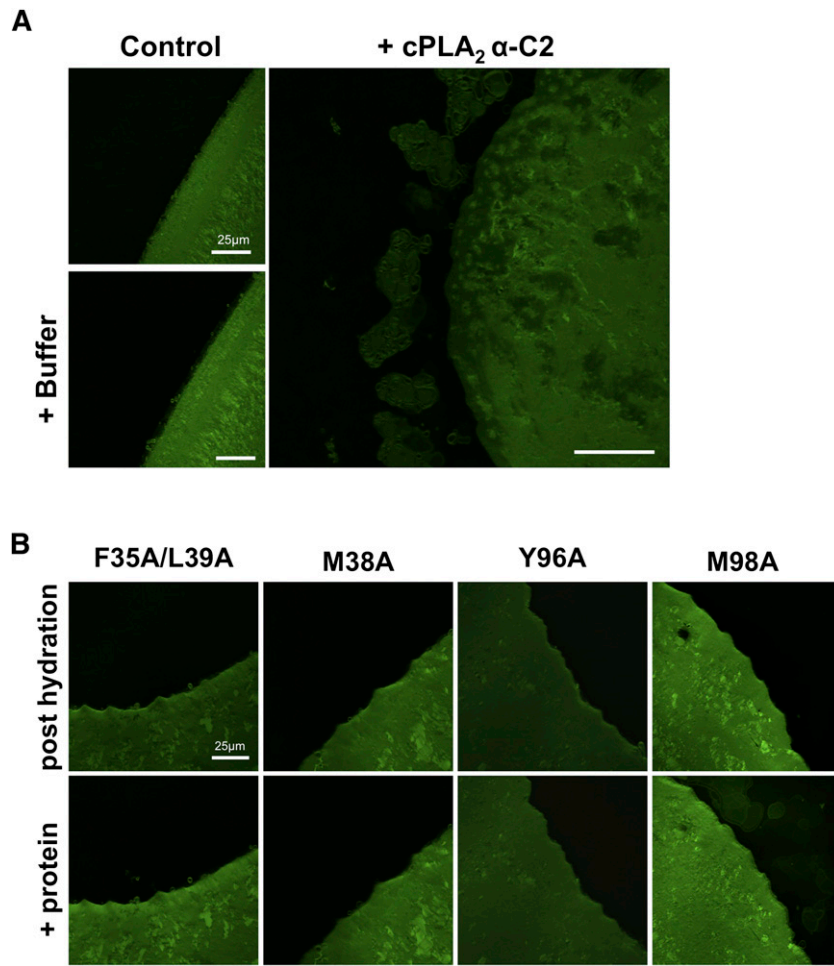
Fig. 4. The C2 domain induces lipid fragmentation of membrane sheets. POPC membrane sheets were used to test the ability of the C2 domain to induce membrane fragmentation to relatively flat membrane surfaces. Membranes were hydrated and then incubated with 2 μM WT or mutant C2 domain for 15 min. A: The WT C2 domain induced extensive membrane fragmentation from membrane sheets, which was not observed in control experiments with buffer alone. B: Hydrophobic and aromatic mutations reduced C2 domain membrane fragmentation. Only M98A displayed detectable membrane fragmentation compared with WT, F35A/L39A, M38A, and Y96A. All membrane sheets were imaged before and after protein incubation. Scale bars = 25 μm.

Membrane penetration and lipid binding affinity of C2 domain and mutations

Membrane penetration of C2 domain and mutations into POPC monolayers was detected by injecting protein into the subphase buffer at varying initial surface pressure (π_0) values (**Fig. 5A, B**). This allows determination of the critical pressure (π_c), which is the pressure up to which the protein penetrates (x-intercept) (35). As previously reported (9, 34), the WT C2 domain robustly penetrated a POPC monolayer with a value of $\sim$36 mN/m. In contrast, F35/L39A and Y96A, which abrogate membrane curvature changes, also significantly reduce the ability of the C2 domain to penetrate POPC monolayers, with π_c values of 23 and 20 mN/m, respectively. In addition, M38A and M98A, which had slightly reduced membrane-deforming capabilities, slightly reduced membrane penetration, with π_c values of 30 and 31 mN/m, respectively. These results demonstrate that the C2 domain can effectively penetrate physiological bilayers because the surface pressure of cell membranes and LUVs is estimated to be in a range of 30–35 mN/m (41). Because monolayer penetration studies with WT and mutants are performed at saturating amounts of protein where maximal binding of WT or mutants occurs, this signifies that, even at saturating conditions of F35A/L39A and Y96A, the proteins are not significantly penetrating into the membrane, whereas M38A and M98A have reduced penetration compared with WT. In the absence of Ca^{2+}, the C2 domain did not insert into the monolayer, and the π_c value of POPC monolayers was essentially undetectable, as previously reported (9, 34). Similarly, the mutation D43N in the C2 domain, which reduces Ca^{2+} binding and was unable to reconstitute FcR-mediated phagocytosis (23), also reduced the π_c value (20 mN/m). Thus, membrane penetration is necessary to induce membrane curvature changes, as observed in the EM, GUV, and membrane sheet assays. Likewise, phosphoinositides are necessary for the ENTH, PH, and ACCH domains to sufficiently penetrate membranes and induce membrane deformation (31, 39, 42).
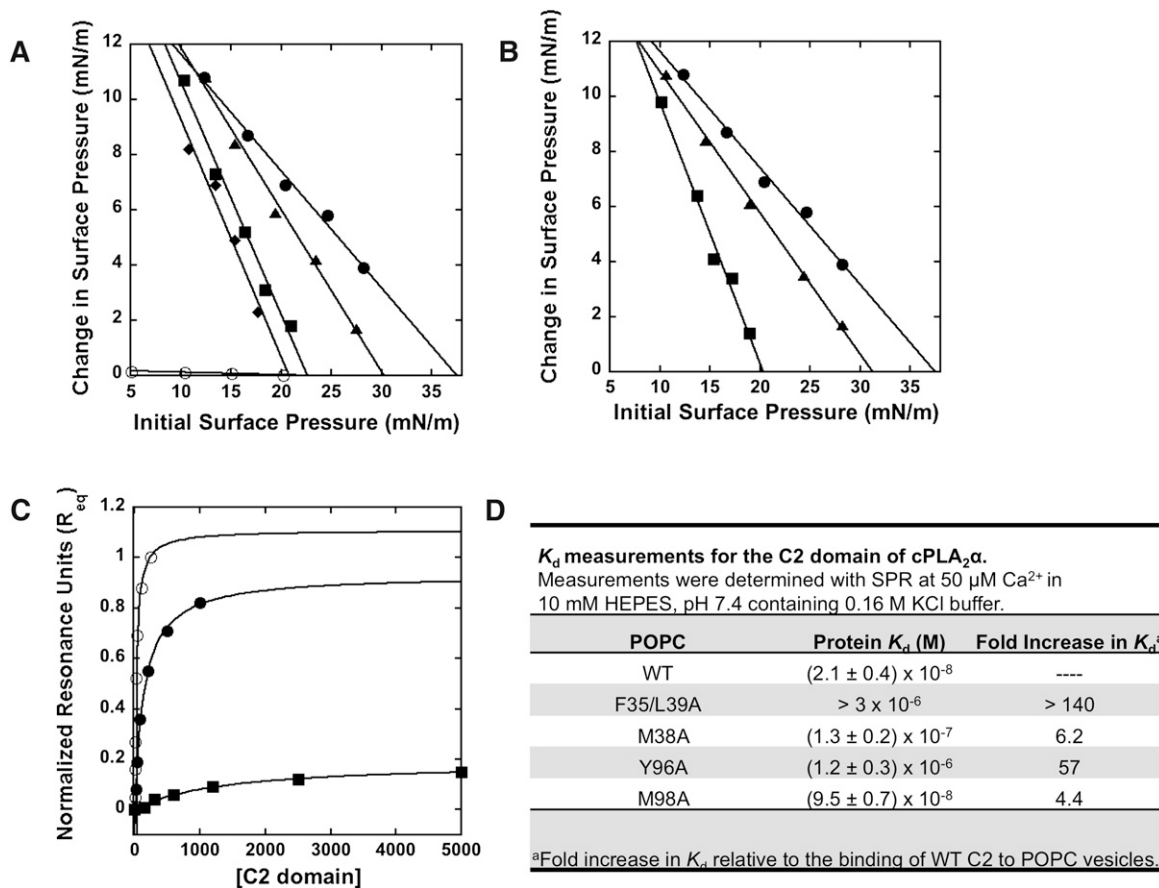
Fig. 5. Mutations that reduce or abrogate membrane deformation reduce or abolish membrane penetration and membrane affinity. A: Insertion of the wild-type C2 domain in the presence of Ca^{2+} (filled circles) or EGTA (open circles) into a POPC monolayer monitored as a function of π_0. Insertion of F35A/L39A (filled squares), M38A (filled triangles), or D43N (filled diamonds) was also monitored in the presence of Ca^{2+}. B: Insertion of the wild-type C2 domain (filled circles), Y96A (filled squares), or M98A (filled triangles). All measurements were performed in the presence of Ca^{2+}. C: The normalized saturation response (R_{eq}) from WT cPLA$_2\alpha$-C2 (filled circles), M38A (filled circles), or Y96A (filled squares) binding at each respective protein concentration was plotted versus C2 to fit with a nonlinear least squares analysis of the binding isotherm $[R_{eq} = R_{max}/(1 + K_d/C)]$ to determine the K_d. D: K_d values for WT and respective mutations binding to POPC vesicles. The binding experiments were completed from independent experiments in triplicate and are listed with their respective $K_d \pm$ SD.

To quantitatively assess the effect of mutations on the ability of the C2 domain to bind POPC vesicles, we performed SPR assays (Fig. 5C, D). A blank surface was used as a control because it has been shown previously that the C2 domain of cPLA$_2\alpha$ does not exhibit nonspecific binding to the L1 chip surface (32, 34). The dissociation constants (K_ds), obtained in triplicate, demonstrate that the C2 domain was associated with 21 ± 4 nM affinity to POPC vesicles at 50 µM CaCl$_2$, but binding was not detectable up to 5 µM in the presence of 100 µM EGTA (data not shown). Mutations that abolish membrane-deforming activity (F35A/L39A and Y96A) demonstrate >140- and 57-fold increases in K_d (Fig. 5D), consistent with their role in membrane penetration and in inducing alterations in membrane structure. Lastly, mutations that slightly reduced membrane curvature changes and membrane penetration (M38A and M98A) increase the K_d by 6.2- and 4.4-fold, respectively. To rule out misfolded C2 domain mutations, we used CD to determine the CD spectra of each mutant in comparison to WT. As shown in supplementary Fig. IA, CD spectras from all mutations overlapped with that of the

WT C2 domain and displayed a spectra indicative of β-sheet with an energy minima at ∼215 nm. To rule out changes in calcium binding for the mutants, we quantified the calcium binding ability of WT, F35A/L39A, M38A, and M98A. Mutations had comparable calcium binding ability to WT, with M38A and M98A displaying slightly reduced binding (not statistically significant) (supplementary Fig. IB). Taken together, our data indicate that membrane affinity of the C2 domain and respective mutations correlates with the ability to penetrate membranes and induce membrane curvature changes.

DISCUSSION

Trafficking of membrane vesicles, endocytosis, and lipid-enveloped viral egress are a few of the cellular pathways where major membrane curvature changes are necessary. These are highly dynamic processes that cannot occur spontaneously because a significant energy barrier has to be overcome to shape the lipid bilayer into a highly curved vesicle (43, 44). To overcome this energy barrier,

protein-mediated effects or lipid bilayer asymmetry can mediate curvature changes. Protein-induced changes are often facilitated by insertion of proteins into the membrane bilayer or scaffolding of proteins on the membrane surface through oligomerization (45). Lipid-mediated changes in bilayer structure can be attributed to lipid asymmetry mediated by cone-shaped and inverted-cone-shaped lipids, where lipid shape can induce positive or negative curvature changes (44).

Membrane curvature changes induced by lipid binding domains were first appreciated with the discovery of the ENTH domain and its ability to induce changes to liposome structure in a PI(4,5)P$_2$-dependent manner (28). The ENTH domain deeply penetrates membranes with a N-terminal amphipathic α-helix and forms oligomers on the membrane (37), both of which are necessary for effective membrane tubulation. This activity is essential to endocytosis and clathrin-coated vesicle formation, which requires substantial changes to plasma membrane structure to form highly curved membrane vesicles (46). Subsequently, the discovery of the BAR domains of amphiphysin (29) and endophilin (47) led to the notion that intrinsic curvature from the crescent moon-shaped BAR domains is essential to remodeling membranes. This led to further investigation, which demonstrated that BAR domains form elegant scaffolds on the membrane where mutation of residues that mediate scaffolding abrogates membrane curvature changes (48, 49). Additionally, as with the ENTH domain, some BAR domains have a N-terminal α-helix that can penetrate into the membrane in addition to a second predicted amphipathic alpha-helix that resides on the membrane binding interface (38). The depth and orientation of this penetration may also be important in regulating membrane curvature changes and membrane fission (50). For instance, it was recently shown that insertion of the amphipathic α-helix drives vesiculation and thus scission by the ENTH domain. In contrast, an antagonistic relationship between the number and length of amphipathic helices in BAR domains was discovered where membrane fission can be restricted by the BAR domains' crescent shape (50). Taken together, depth and area of insertion as well as inherent protein scaffold shape play a critical role in the type of membrane curvature generated and whether or not membrane fission will proceed.

PH domains (30) and C2 domains (32) have also been shown to induce membrane curvature changes. The FAPP1 and 2 PH domains require insertion of a turret loop adjacent to the PI(4)P binding pocket (42) to induce membrane remodeling where the inherent shape of FAPP1 or -2 may also play a critical role (30). However, unlike the ENTH and BAR domain, elegant models of membrane scaffolding and modes of membrane curvature induction for PH and C2 domains have not been investigated. In addition, the relationship between membrane penetration of C2 domains and membrane curvature changes is unknown. Recently, it was shown that the C2B domain alone or the tandem C2AC2B domains of synaptotagmin 1, which can induce membrane tubulation (32)

and vesicle aggregation (51), could induce lipid demixing of PS in POPC:POPS vesicles (52), which is thought to induce positive bilayer curvature changes.

Here we demonstrate that the C2 domain of cPLA$_2$α, long appreciated as a high-affinity target for zwitterionic lipids (9) with an ability to deeply penetrate the hydrocarbon core of zwitterionic membranes, is able to induce substantial changes to membrane structure. Imaging of liposomes with TEM, GUVs with confocal microscopy, or membrane sheets with confocal microscopy demonstrated dramatic changes in membrane structure induced in a Ca^{2+}-dependent manner by the cPLA$_2$α C2 domain. Detectable changes in membrane structure correlated strongly with membrane penetrating ability and lipid binding affinity. Membrane penetration of the C2 domain generated positive membrane curvature, as evidenced in the TEM and confocal assays (**Fig. 6**). Positive curvature generation by the C2 domain is consistent with the role of cPLA$_2$α in formation of the phagosome, Golgi tubulation, and Golgi vesiculation, which occur by budding into the cytoplasm. The protein concentrations of C2 domain used in the membrane curvature assays were similar or lower than most of the previous studies in the literature (28, 29, 32), supporting the specific nature of our findings. For the C2 domain, there may be a threshold affinity and depth or extent of penetration that is responsible for generating curvature because M38A and M98A, which reduced membrane penetration and affinity, induced statistically significant changes in membrane curvature. In the sheet assay, M38A did not induce detectable membrane fragmentation, whereas M98A did. M38A is located in CBL1 and has lower affinity than M98A, which is located in CBL3
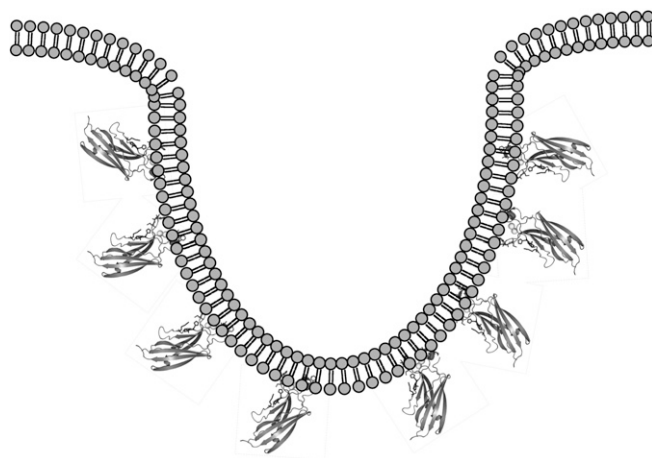

Fig. 6. Membrane penetration by the C2 domain of cPLA$_2$α is sufficient to induce membrane curvature changes. The hydrophobic residues essential in penetrating the membrane are also key for membrane curvature generation. The deep ~15 Å penetration of these hydrophobic and aliphatic residues as well as a significant area of insertion (~2110 Å^2) are sufficient to reduce the energetic barrier to bend the membrane as deletion of one of these key residues abolishes this effect, as shown for the F35A/L39A and Y96A mutants. Although the overall mechanism is unknown, our data suggest that membrane penetration of the C2 domain is vital for membrane bending, tubulation, vesiculation, and fragmentation, depending on the initial curvature of the membrane.

(Fig. 1). It has been shown that CBL1 penetrates more deeply into the bilayer than CBL3 (53), which could perhaps play a role in the different observations in the membrane sheet assays. Although the origin of this discrepancy is unknown, it leaves room for extensive biophysical studies of C2 domain parameters required for membrane curvature generation. It also appears that M38A and M98A may cause some vesiculation in the liposome assays, as visualized by EM, as well as differences in the extent of vesiculation in the GUV assays, suggesting that the depth of penetration and/or membrane affinity may play an important role in the type of membrane curvature or membrane reorganization that is generated. Studying the C2 domain's role in the type of curvature generation in conjunction with membrane fission (50) will be essential to improve our understanding of the mechanism of curvature generation for this C2 domain. Penetration of hydrophobic residues by the C2 domain occurs into the hydrocarbon layer ($\sim$15 Å), reminiscent of the ENTH domain (37, 39), so it is possible that membrane fission and vesiculation (50) may occur, which is supported by membrane fragmentation in the membrane sheet assays. C2 domains and PH domains may also induce different types of curvature. For instance, in this study, the C2 domain induced membrane fragmentation, whereas studies with PH domains have demonstrated extensive positive curvature induction in the form of tubules in the membrane sheet assays (42).

Future studies need to consider the role of C2 domain membrane binding and penetration in inducing or contributing to membrane curvature changes in conjunction with cPLA$_2\alpha$ activity. The fact that the C2 domain alone is able to reconstitute FcR-mediated phagocytosis (23) suggests that the cPLA$_2\alpha$ C2 domain has a high membrane remodeling activity that is essential to membrane reorganization. Additionally, inhibition of cPLA$_2\alpha$ activity in cells with the inhibitor pyrrophenone generated an allosteric block that prevented cPLA$_2\alpha$ translocation (23), which does not allow one to account for C2 membrane binding and insertion in assessing the generation of lysophospholipids in curvature generation (26). Nonetheless, the prior study demonstrated the C2 domain process is Ca^{2+} dependent because D43N, which abrogates calcium binding, could not reconstitute phagocytosis. In conjunction with the current study, this strongly suggests that membrane penetration of the C2 domain is necessary for these effects because calcium is required for membrane penetration of the C2 domain (Fig. 1C and 5A) (9). It is also now well established that the cationic β-groove of the C2 domain binds C1P (21), which is important for cPLA$_2\alpha$ activity (21) and cellular translocation (54). Additionally, the role of ceramide kinase and its product C1P are key players in phagocytosis (55, 56). Thus, it has been hypothesized that C1P has an important role in recruitment of cPLA$_2\alpha$ in phagocytosis (57). To this end, it is tempting to speculate that cPLA$_2\alpha$ may be able to induce reorganization or clustering of membranes harboring C1P.

The surface area of insertion for the C2 domain (58) is more substantial than that of the ENTH (39, 50) and PH domains (59), at least for a monomer; however, this alone may not account for the membrane-mediated curvature changes. It was first thought that the N-terminal α-helix insertion for ENTH domains, and to some degree for BAR domains, was the major cause of the membrane curvature induction. However, more recent and sophisticated studies have demonstrated the ability of these proteins to scaffold on the membrane (48, 49). This scaffolding is essential for in vitro and cellular observations of membrane curvature changes (48, 49). Future studies need to be directed toward resolving the molecular details of C2 oligomerization as well as the role of β-groove C1P binding in membrane curvature changes or membrane reorganization. Additionally, the type of membrane curvature generated by the C2 domain as well as full-length cPLA$_2\alpha$ will require extensive analysis using a combination of biophysical, biochemical, and cellular assays. Investigating how the C2 domain insertion and catalytic domain generation of lysophospholipids contribute to in vitro and cellular membrane curvature changes should solve a number of questions in the fields of membrane trafficking and phagosome formation.

The type of curvature generated by the C2 domain or full-length enzyme may also be key to normal and aberrant physiological processes linked to cPLA$_2\alpha$ activity. cPLA$_2\alpha$ has been shown to function in generation of cholesterol-rich, GPI protein-containing endosomes (26), Golgi tubulation and vesiculation (24, 25), and Golgi-to-PM trafficking (60). Additionally, cPLA$_2\alpha$ association with the Golgi has been shown to regulate the function of endothelial cells (61, 62), which serve a barrier function in the luminal surfaces of blood vessels. Proliferation of endothelial cells has been shown to occur for the formation of blood vessels in wound healing and tumor formation while blocking cPLA$_2\alpha$ activity through an inhibitor or siRNA blocks endothelial cell proliferation and cell cycle entry (61). In terms of pathophysiological states, cPLA$_2\alpha$ has been linked to diseases such as asthma (4), arthritis (6), and cancers (5). Thus, up- or down-regulation of cPLA$_2\alpha$ enzyme levels may alter the transport of vesicles from the Golgi to the PM, modify intra-Golgi transport, or effect endothelial barrier function through the combined generation of fatty acids and lysophospholipids and membrane penetration of the C2 domain of cPLA$_2\alpha$. Additionally, because cPLA$_2\alpha$ enzyme inhibitors act as an allosteric block that reduces or precludes cPLA$_2\alpha$ membrane translocation, it is difficult to rule out the C2 domain-mediated effects. Thus, our data support a model where vesiculation or tubulation of the Golgi may occur in response to C2 domain membrane penetration of the full-length enzyme under conditions of low cPLA$_2\alpha$ activity. Linkage of biochemical and biophysical studies in vitro and in cells with cellular and disease models that can tease apart the role of C2 domain penetration and cPLA$_2\alpha$ activity in these processes will be key to unraveling the full mechanism of membrane curvature generation.

REFERENCES

1. Clark, J. D., A. R. Schievella, E. A. Nalefski, and L. L. Lin. 1995. Cytosolic phospholipase A2. *J. Lipid Mediat. Cell Signal.* **12:** 83–117.
2. Leslie, C. C., T. A. Gangelhoff, and M. H. Gelb. 2010. Localization and function of cytosolic phospholipase A2alpha at the Golgi. *Biochimie.* **92:** 620–626.

3. Shimizu, T., T. Ohto, and Y. Kita. 2006. Cytosolic phospholipase A2: biochemical properties and physiological roles. *IUBMB Life.* **58:** 328–333.

4. Hewson, C. A., S. Patel, L. Calzetta, H. Campwala, S. Havard, E. Luscombe, P. A. Clarke, P. T. Peachell, M. G. Matera, M. Cazzola, et al. 2012. Preclinical evaluation of an inhibitor of cytosolic phospholipase A2alpha for the treatment of asthma. *J. Pharmacol. Exp. Ther.* **340:** 656–665.

5. Sundarraj, S., S. Kannan, R. Thangam, and P. Gunasekaran. 2012. Effects of the inhibition of cytosolic phospholipase A(2)alpha in non-small cell lung cancer cells. *J. Cancer Res. Clin. Oncol.* **138:** 827–835.

6. Tai, N., K. Kuwabara, M. Kobayashi, K. Yamada, T. Ono, K. Seno, Y. Gahara, J. Ishizaki, and Y. Hori. 2010. Cytosolic phospholipase A2 alpha inhibitor, pyrroxyphene, displays anti-arthritic and anti-bone destructive action in a murine arthritis model. *Inflamm. Res.* **59:** 53–62.

7. Kishimoto, K., R. C. Li, J. Zhang, J. A. Klaus, K. K. Kibler, S. Dore, R. C. Koehler, and A. Sapirstein. 2010. Cytosolic phospholipase A2 alpha amplifies early cyclooxygenase-2 expression, oxidative stress and MAP kinase phosphorylation after cerebral ischemia in mice. *J. Neuroinflammation.* **7:** 42.

8. Kerkela, R., M. Boucher, R. Zaka, E. Gao, D. Harris, J. Piuhola, J. Song, R. Serpi, K. C. Woulfe, J. Y. Cheung, et al. 2011. Cytosolic phospholipase A(2)alpha protects against ischemia/reperfusion injury in the heart. *Clin. Transl. Sci.* **4:** 236–242.

9. Bittova, L., M. Sumandea, and W. Cho. 1999. A structure-function study of the C2 domain of cytosolic phospholipase A2. Identification of essential calcium ligands and hydrophobic membrane binding residues. *J. Biol. Chem.* **274:** 9665–9672.

10. Corbin, J. A., J. H. Evans, K. E. Landgraf, and J. J. Falke. 2007. Mechanism of specific membrane targeting by C2 domains: localized pools of target lipids enhance Ca2+ affinity. *Biochemistry.* **46:** 4322–4336.

11. Tucker, D. E., M. Ghosh, F. Ghomashchi, R. Loper, S. Suram, B. S. John, M. Girotti, J. G. Bollinger, M. H. Gelb, and C. C. Leslie. 2009. Role of phosphorylation and basic residues in the catalytic domain of cytosolic phospholipase A2alpha in regulating interfacial kinetics and binding and cellular function. *J. Biol. Chem.* **284:** 9596–9611.

12. Evans, J. H., and C. C. Leslie. 2004. The cytosolic phospholipase A2 catalytic domain modulates association and residence time at Golgi membranes. *J. Biol. Chem.* **279:** 6005–6016.

13. Evans, J. H., D. M. Spencer, A. Zweifach, and C. C. Leslie. 2001. Intracellular calcium signals regulating cytosolic phospholipase A2 translocation to internal membranes. *J. Biol. Chem.* **276:** 30150–30160.

14. Das, S., and W. Cho. 2002. Roles of catalytic domain residues in interfacial binding and activation of group IV cytosolic phospholipase A2. *J. Biol. Chem.* **277:** 23838–23846.

15. Murray, D., and B. Honig. 2002. Electrostatic control of the membrane targeting of C2 domains. *Mol. Cell.* **9:** 145–154.

16. Frazier, A. A., M. A. Wisner, N. J. Malmberg, K. G. Victor, G. E. Fanucci, E. A. Nalefski, J. J. Falke, and D. S. Cafiso. 2002. Membrane orientation and position of the C2 domain from cPLA2 by site-directed spin labeling. *Biochemistry.* **41:** 6282–6292.

17. Pettus, B. J., A. Bielawska, P. Subramanian, D. S. Wijesinghe, M. Maceyka, C. C. Leslie, J. H. Evans, J. Freiberg, P. Roddy, Y. A. Hannun, et al. 2004. Ceramide 1-phosphate is a direct activator of cytosolic phospholipase A2. *J. Biol. Chem.* **279:** 11320–11326.

18. Subramanian, P., R. V. Stahelin, Z. Szulc, A. Bielawska, W. Cho, and C. E. Chalfant. 2005. Ceramide 1-phosphate acts as a positive allosteric activator of group IVA cytosolic phospholipase A2 alpha and enhances the interaction of the enzyme with phosphatidylcholine. *J. Biol. Chem.* **280:** 17601–17607.

19. Balsinde, J., M. A. Balboa, W. H. Li, J. Llopis, and E. A. Dennis. 2000. Cellular regulation of cytosolic group IV phospholipase A2 by phosphatidylinositol bisphosphate levels. *J. Immunol.* **164:** 5398–5402.

20. Mosior, M., D. A. Six, and E. A. Dennis. 1998. Group IV cytosolic phospholipase A2 binds with high affinity and specificity to phosphatidylinositol 4,5-bisphosphate resulting in dramatic increases in activity. *J. Biol. Chem.* **273:** 2184–2191.

21. Stahelin, R. V., P. Subramanian, M. Vora, W. Cho, and C. E. Chalfant. 2007. Ceramide-1-phosphate binds group IVA cytosolic phospholipase a2 via a novel site in the C2 domain. *J. Biol. Chem.* **282:** 20467–20474.

22. Casas, J., M. A. Gijon, A. G. Vigo, M. S. Crespo, J. Balsinde, and M. A. Balboa. 2006. Phosphatidylinositol 4,5-bisphosphate anchors cytosolic group IVA phospholipase A2 to perinuclear membranes and decreases its calcium requirement for translocation in live cells. *Mol. Biol. Cell.* **17:** 155–162.

23. Zizza, P., C. Iurisci, M. Bonazzi, P. Cossart, C. C. Leslie, D. Corda, and S. Mariggio. 2012. Phospholipase A2IValpha regulates phagocytosis independent of its enzymatic activity. *J. Biol. Chem.* **287:** 16849–16859.

24. Grimmer, S., M. Ying, S. Walchli, B. van Deurs, and K. Sandvig. 2005. Golgi vesiculation induced by cholesterol occurs by a dynamin- and cPLA2-dependent mechanism. *Traffic.* **6:** 144–156.

25. San Pietro, E., M. Capestrano, E. V. Polishchuk, A. DiPentima, A. Trucco, P. Zizza, S. Mariggio, T. Pulvirenti, M. Sallese, S. Tete, et al. 2009. Group IV phospholipase A(2)alpha controls the formation of inter-cisternal continuities involved in intra-Golgi transport. *PLoS Biol.* **7:** e1000194.

26. Cai, B., S. Caplan, and N. Naslavsky. 2012. cPLA2alpha and EHD1 interact and regulate the vesiculation of cholesterol-rich, GPI-anchored, protein-containing endosomes. *Mol. Biol. Cell.* **23:** 1874–1888.

27. Campelo, F., H. T. McMahon, and M. M. Kozlov. 2008. The hydrophobic insertion mechanism of membrane curvature generation by proteins. *Biophys. J.* **95:** 2325–2339.

28. Ford, M. G., I. G. Mills, B. J. Peter, Y. Vallis, G. J. Praefcke, P. R. Evans, and H. T. McMahon. 2002. Curvature of clathrin-coated pits driven by epsin. *Nature.* **419:** 361–366.

29. Peter, B. J., H. M. Kent, I. G. Mills, Y. Vallis, P. J. Butler, P. R. Evans, and H. T. McMahon. 2004. BAR domains as sensors of membrane curvature: the amphiphysin BAR structure. *Science.* **303:** 495–499.

30. Cao, X., U. Coskun, M. Rossle, S. B. Buschhorn, M. Grzybek, T. R. Dafforn, M. Lenoir, M. Overduin, and K. Simons. 2009. Golgi protein FAPP2 tubulates membranes. *Proc. Natl. Acad. Sci. USA.* **106:** 21121–21125.

31. Heller, B., E. Adu-Gyamfi, W. Smith-Kinnaman, C. Babbey, M. Vora, Y. Xue, R. Bittman, R. V. Stahelin, and C. D. Wells. 2010. Amot recognizes a juxtanuclear endocytic recycling compartment via a novel lipid binding domain. *J. Biol. Chem.* **285:** 12308–12320.

32. Martens, S., M. M. Kozlov, and H. T. McMahon. 2007. How synaptotagmin promotes membrane fusion. *Science* **316:** 1205–1208.

33. Hom, R. A., M. Vora, M. Regner, O. M. Subach, W. Cho, V. V. Verkhusha, R. V. Stahelin, and T. G. Kutateladze. 2007. pH-dependent binding of the Epsin ENTH domain and the AP180 ANTH domain to PI(4,5)P2-containing bilayers. *J. Mol. Biol.* **373:** 412–423.

34. Stahelin, R. V., and W. Cho. 2001. Roles of calcium ions in the membrane binding of C2 domains. *Biochem. J.* **359:** 679–685.

35. Cho, W., L. Bittova, and R. V. Stahelin. 2001. Membrane binding assays for peripheral proteins. *Anal. Biochem.* **296:** 153–161.

36. Stahelin, R. V., D. Karathanassis, D. Murray, R. L. Williams, and W. Cho. 2007. Structural and membrane binding analysis of the PX domain of Bem1p: basis of phosphatidylinositol-4-phosphate specificity. *J. Biol. Chem.* **282:** 25737–25747.

37. Yoon, Y., J. Tong, P. J. Lee, A. Albanese, N. Bhardwaj, M. Kallberg, M. A. Digman, H. Lu, E. Gratton, Y. K. Shin, et al. 2010. Molecular basis of the potent membrane-remodeling activity of the epsin 1 N-terminal homology domain. *J. Biol. Chem.* **285:** 531–540.

38. Gallop, J. L., C. C. Jao, H. M. Kent, P. J. Butler, P. R. Evans, R. Langen, and H. T. McMahon. 2006. Mechanism of endophilin N-BAR domain-mediated membrane curvature. *EMBO J.* **25:** 2898–2910.

39. Stahelin, R. V., F. Long, B. J. Peter, D. Murray, P. De Camilli, H. T. McMahon, and W. Cho. 2003. Contrasting membrane interaction mechanisms of AP180 N-terminal homology (ANTH) and epsin N-terminal homology (ENTH) domains. *J. Biol. Chem.* **278:** 28993–28999.

40. Shnyrova, A. V., J. Ayllon, I. I. Mikhalyov, E. Villar, J. Zimmerberg, and V. A. Frolov. 2007. Vesicle formation by self-assembly of membrane-bound matrix proteins into a fluidlike budding domain. *J. Cell Biol.* **179:** 627–633.

41. Blume, A. 1979. A comparative study of the phase transitions of phospholipid bilayers and monolayers. *Biochim. Biophys. Acta.* **557:** 32–44.

42. He, J., J. L. Scott, A. Heroux, S. Roy, M. Lenoir, M. Overduin, R. V. Stahelin, and T. G. Kutateladze. 2011. Molecular basis of phosphatidylinositol 4-phosphate and ARF1 GTPase recognition by the FAPP1 pleckstrin homology (PH) domain. *J. Biol. Chem.* **286:** 18650–18657.

43. Baumgart, T., B. R. Capraro, C. Zhu, and S. L. Das. 2011. Thermodynamics and mechanics of membrane curvature generation and sensing by proteins and lipids. *Annu. Rev. Phys. Chem.* **62:** 483–506.

44. Kooijman, E. E., V. Chupin, N. L. Fuller, M. M. Kozlov, B. de Kruijff, K. N. Burger, and P. R. Rand. 2005. Spontaneous curvature of phosphatidic acid and lysophosphatidic acid. *Biochemistry.* **44:** 2097–2102.

45. Graham, T. R., and M. M. Kozlov. 2010. Interplay of proteins and lipids in generating membrane curvature. *Curr. Opin. Cell Biol.* **22:** 430–436.

46. McMahon, H. T., and E. Boucrot. 2011. Molecular mechanism and physiological functions of clathrin-mediated endocytosis. *Nature. Rev. Mol. Cell. Biol.* **12:** 517–533.

47. Gallop, J. L., P. J. Butler, and H. T. McMahon. 2005. Endophilin and CtBP/BARS are not acyl transferases in endocytosis or Golgi fission. *Nature.* **438:** 675–678.

48. Frost, A., R. Perera, A. Roux, K. Spasov, O. Destaing, E. H. Egelman, P. De Camilli, and V. M. Unger. 2008. Structural basis of membrane invagination by F-BAR domains. *Cell.* **132:** 807–817.

49. Shimada, A., H. Niwa, K. Tsujita, S. Suetsugu, K. Nitta, K. Hanawa-Suetsugu, R. Akasaka, Y. Nishino, M. Toyama, L. Chen, et al. 2007. Curved EFC/F-BAR-domain dimers are joined end to end into a filament for membrane invagination in endocytosis. *Cell.* **129:** 761–772.

50. Boucrot, E., A. Pick, G. Camdere, N. Liska, E. Evergren, H. T. McMahon, and M. M. Kozlov. 2012. Membrane fission is promoted by insertion of amphipathic helices and is restricted by crescent BAR domains. *Cell.* **149:** 124–136.

51. Arac, D., X. Chen, H. A. Khant, J. Ubach, S. J. Ludtke, M. Kikkawa, A. E. Johnson, W. Chiu, T. C. Sudhof, and J. Rizo. 2006. Close membrane-membrane proximity induced by Ca(2+)-dependent multivalent binding of synaptotagmin-1 to phospholipids. *Nat. Struct. Mol. Biol.* **13:** 209–217.

52. Lai, A. L., L. K. Tamm, J. F. Ellena, and D. S. Cafiso. 2011. Synaptotagmin 1 modulates lipid acyl chain order in lipid bilayers by demixing phosphatidylserine. *J. Biol. Chem.* **286:** 25291–25300.

53. Malmberg, N. J., D. R. Van Buskirk, and J. J. Falke. 2003. Membrane-docking loops of the cPLA2 C2 domain: detailed structural analysis of the protein-membrane interface via site-directed spin-labeling. *Biochemistry.* **42:** 13227–13240.

54. Lamour, N. F., P. Subramanian, D. S. Wijesinghe, R. V. Stahelin, J. V. Bonventre, and C. E. Chalfant. 2009. Ceramide 1-phosphate is required for the translocation of group IVA cytosolic phospholipase A2 and prostaglandin synthesis. *J. Biol. Chem.* **284:** 26897–26907.

55. Hinkovska-Galcheva, V., L. A. Boxer, A. Kindzelskii, M. Hiraoka, A. Abe, S. Goparju, S. Spiegel, H. R. Petty, and J. A. Shayman. 2005. Ceramide 1-phosphate, a mediator of phagocytosis. *J. Biol. Chem.* **280:** 26612–26621.

56. Hinkovska-Galcheva, V. T., L. A. Boxer, P. J. Mansfield, D. Harsh, A. Blackwood, and J. A. Shayman. 1998. The formation of ceramide-1-phosphate during neutrophil phagocytosis and its role in liposome fusion. *J. Biol. Chem.* **273:** 33203–33209.

57. Falke, J. J. 2012. Lipid targeting domain with dual-membrane specificity that expands the diversity of intracellular targeting reactions. *Proc. Natl. Acad. Sci. USA.* **109:** 1816–1817.

58. Malkova, S., F. Long, R. V. Stahelin, S. V. Pingali, D. Murray, W. Cho, and M. L. Schlossman. 2005. X-ray reflectivity studies of cPLA2{alpha}-C2 domains adsorbed onto Langmuir monolayers of SOPC. *Biophys. J.* **89:** 1861–1873.

59. Lenoir, M., U. Coskun, M. Grzybek, X. Cao, S. B. Buschhorn, J. James, K. Simons, and M. Overduin. 2010. Structural basis of wedging the Golgi membrane by FAPP pleckstrin homology domains. *EMBO Rep.* **11:** 279–284.

60. Choukroun, G. J., V. Marshansky, C. E. Gustafson, M. McKee, R. J. Hajjar, A. Rosenzweig, D. Brown, and J. V. Bonventre. 2000. Cytosolic phospholipase A$_2$ regulates Golgi structure and modulates intracellular trafficking of membrane proteins. *J. Clin. Invest.* **106:** 983–993.

61. Herbert, S. P., S. Ponnambalam, and J. H. Walker. 2005. Cytosolic phospholipase A$_2$-α mediates endothelial cell proliferation and is inactivated by association with the Golgi apparatus. *Mol. Biol. Cell.* **16:** 3800–3809.

62. Herbert, S. P., A. F. Odell, S. Ponnambalam, and J. H. Walker. 2007. The confluence-dependent interaction of cytosolic phospholipase A$_2$-α with annexin A1 regulates endothelial cell prostaglandin E2 generation. *J. Biol. Chem.* **282:** 34468–34478.